

Title	Pyrolytic transformation from polydihydrosilane to hydrogenated amorphous silicon film
Author(s)	Masuda, Takashi; Matsuki, Yasuo; Shimoda, Tatsuya
Citation	Thin Solid Films, 520(21): 6603-6607
Issue Date	2012-07-16
Type	Journal Article
Text version	author
URL	http://hdl.handle.net/10119/11459
Rights	NOTICE: This is the author's version of a work accepted for publication by Elsevier. Takashi Masuda, Yasuo Matsuki, Tatsuya Shimoda, Thin Solid Films, 520(21), 2012, 6603-6607, http://dx.doi.org/10.1016/j.tsf.2012.07.028
Description	

1 **Pyrolytic Transformation from Polydihydrosilane to Hydrogenated Amorphous**
2 **Silicon Film**

3 Takashi Masuda ^a, Yasuo Matsuki ^{a,c}, Tatsuya Shimoda ^{a,b}

4 ^a Japan Science and Technology Agency, ERATO, Shimoda Nano-Liquid Process
5 Project, 2-13 Asahidai, Nomi, Ishikawa, 923-1211, Japan

6 ^b School of Materials Science, Japan Advanced Institute of Science and Technology,
7 1-1 Asahidai, Nomi, Ishikawa, 923-1292, Japan

8 ^c Yokkaichi Research Center, JSR Corporation, 100 Kawajiri-cho, Yokkaichi, Mie,
9 510-8552, Japan.

10
11 **Abstract**

12 The fabrication of thin film silicon devices based on solution processes rather than on
13 conventional vacuum processes is of substantial interest since cost reductions may result.
14 Using a solution process, we coated substrates with polydihydrosilane solution and
15 studied the pyrolytic transformation of the material into hydrogenated amorphous
16 silicon (a-Si:H). From thermal gravimetry and differential thermal analysis data a
17 significant reduction in weight of the material and a construction of Si-Si bonds are
18 concluded for the pyrolysis temperature $T_p = 270$ to 360 °C. The appearance of
19 amorphous silicon phonon bands in Raman spectra for films prepared at $T_p \geq 330$ °C
20 suggests the construction of a three-dimensional amorphous silicon network. Films
21 prepared at $T_p \geq 360$ °C exhibit a hydrogen content near 10 at.% and an optical gap near
22 1.6 eV similar to device-grade vacuum processed a-Si:H. However, the infrared
23 microstructure factor, the spin density, and the photosensitivity require significant
24 improvements.

25
26 **Keywords:** CPS, cyclopentasilane, polydihydrosilane, polysilane, amorphous silicon,
27 solution process.

30 **1. Introduction**

31 Hydrogenated amorphous silicon (a-Si:H) films have received considerable
32 interest because of their immense potential for various application in large-area
33 electronic devices such as solar cells and thin-film transistors [1,2]. To date, a-Si:H
34 films are deposited using expensive vacuum-based equipment and high amounts of
35 dangerous and expensive silicon-based gases. These are factors making cost reduction
36 and large-area film deposition difficult. If a-Si:H films can be deposited using liquid
37 state silicon materials and inexpensive vacuum-free equipments, this situation might
38 change drastically. Previously, we have reported on synthesis of silicon precursor
39 solutions consisting of polydihydrosilane ($-(\text{SiH}_2)_n-$) and an organic solvent and
40 demonstrated the realization of solution-processed (Sol.P) poly-silicon films [3] using
41 spin-coat and ink-jet methods. Furthermore, we have demonstrated the Sol.P a-Si:H
42 solar cell using spin-coat method [4]. The fabrication process involved the pyrolysis of
43 polydihydrosilane followed by a spontaneous formation of a three-dimensional silicon
44 network releasing a high amount of gases (H_2 and SiH_x). Pyrolysis experiments of
45 silicon containing polymers with a purpose to fabricate efficient emitters in the UV to
46 IR spectral range for light emitting diodes have been reported recently [5]. However,
47 systematic studies for the Sol.P a-Si:H films were not reported so far. The aim of the
48 present research is the study of the pyrolytic transformation from a polydihydrosilane
49 liquid film to an a-Si:H solid film by changing the pyrolysis temperature T_p from 270 to
50 420 °C employing a fixed heating time of 15 min. To examine the pyrolytic
51 transformation, thermal gravimetry (TG) and differential thermal analysis (DTA),
52 Raman scattering, Fourier-transform infrared spectroscopy (FT-IR), and secondary ion
53 mass spectroscopy (SIMS) measurements are applied. To characterize the electrical
54 properties of Sol.P films, transmittance and reflectance spectroscopy in the UV–visible
55 range (UV–VIS TR), electron spin resonance (ESR), and photoconductivity/dark
56 conductivity measurements are carried out.

57

58 **2. Experiment**

59 **2.1 Preparation of Sol.P films**

60 Polydihydrosilane was synthesised by a photo-induced ring-opening

61 polymerization process of cyclopentasilane (Si_5H_{10} ;CPS) [6] employing the Kipping
62 method [7,8]. The polydihydrosilane dissolved in cyclooctane at the concentration of
63 10–20 wt. % was spin-coated on quartz or silicon substrates under similar conditions as
64 in previous work [9] in which we explored the stability of polydihydrosilane liquid
65 films on various solid substrates. The pyrolysis of the polydihydrosilane was carried out
66 at $T_p = 270$ to 420 °C using a fixed heating time of 15 min. The samples were set on a
67 hot plate in a glove box filled with nitrogen gas in order to avoid reaction with air, as
68 CPS and polydihydrosilane easily ignite in air. The oxygen and the dew point in the
69 glove box were less than 0.5 ppm and -75 °C, respectively.

70

71 **2.2 Characterization**

72 The thermal analysis of polydihydrosilane was carried out using TG/DTA
73 (EXTAR TGDTA6200 by Seiko Instruments Inc.) which was installed in the glove box.
74 Inactive Al_2O_3 was selected as a sample pan. Approximately 20–30 mg of
75 polydihydrosilane was added dropwise on the pan. To prevent as much oxidation as
76 possible during the measurement, the purge gas was purified via a gas purifier (by
77 Pureron Japan Co. Ltd.) to obtain oxygen concentrations < 1 ppb, and a relatively high
78 flow rate of 200 mL/min was employed. The polydihydrosilane was heated in the
79 temperature range between 25 and 450 °C with the heating rate of 10 °C/min.

80 The low-frequency phonon bands of the a-Si network and the local vibration of the
81 SiH_n groups in the network were probed by Raman scattering (Ramascope by
82 Renishaw) and FT-IR (ALPHA by Bruker Optics), respectively.

83 In addition to IR spectral analysis, SIMS (model-6300 by PHI) was applied to
84 quantify the hydrogen and oxygen content. A 3.0 KeV Cs^+ primary ion beam with an
85 impact angle of 60° with respect to surface normal was used and negative secondary
86 ions were detected. Charge build-up during profiling was compensated for by use of an
87 electron gun with an intensity of 0.75 KeV.

88 To determine the optical gap E_g and spin density N_S , we used UV-VIS TR
89 (FilmTek-3000 by Scientific Computing International) and ESR (JES-FA100 by JEOL
90 Ltd.), respectively. An AM-1.5G solar simulator (WXS-50S by WACOM Electric Co.
91 Ltd.) with an intensity of $100\text{mW}/\text{cm}^2$ was adopted for the illuminated current and

92 voltage measurement. The conductivity was measured on a coplanar configuration of
93 250 μm gap width, using aluminum contacts for samples. The dark conductivity σ_d and
94 the photoconductivity σ_p were measured at room temperature for the films prepared at
95 various T_p .

96

97 **3. Results and discussion**

98 **3.1 Photographic image of Sol.P films and TG/DTA results**

99 Fig. 1 shows photographic image of Sol.P films with a thickness of 50 nm, coated
100 on quartz substrate $2 \times 2 \text{ cm}^2$ in size and pyrolysed at temperatures between $T_p < 270$
101 and $T_p = 420 \text{ }^\circ\text{C}$. The films prepared at $T_p \leq 270 \text{ }^\circ\text{C}$ are transparent, and a drastic change
102 from transparent to yellow color appears when T_p is increased from 270 to 300 $^\circ\text{C}$. This
103 change in color can be attributed to a reduction of E_g from that of polydihydrosilane of
104 6.5 eV [10] to lower values. The transparency of films prepared at $T_p \leq 270 \text{ }^\circ\text{C}$
105 corresponds to an insulator material whereas the yellow and brown color of films
106 pyrolysed at $T_p = 300\text{--}420 \text{ }^\circ\text{C}$ indicates the presence of semiconductor materials. From
107 this, a transformation from a polymer to an amorphous semiconductor can be concluded
108 to occur near $T_p = 270 \text{ }^\circ\text{C}$.

109 To study the pyrolysis directly, TG and DTA measurements of polydihydrosilane
110 were carried out. Fig. 2 shows the TG signal (bold solid line) and the DTA signal (thin
111 solid line) as a function of heating temperature T_h . Also shown is the temperature/time
112 derivative DTG (dashed line) of the TG signal.

113 The TG data indicate a weight loss of about 58 % by heating up to 360 $^\circ\text{C}$ and
114 consequently only 42 % of the material remained in the form of hydrogenated
115 amorphous silicon. In agreement with thermal desorption spectroscopy (TDS)
116 measurements [3] one may assume that the weight reduction is caused by desorption of
117 H_2 and SiH_x . According to the DTG curves the major weight loss takes place at $T = 100$,
118 200, and 300 $^\circ\text{C}$. A broad exothermal peak is found in the DTA signal extending from
119 80 to 450 $^\circ\text{C}$ with a maximum near 320 $^\circ\text{C}$. These results suggest that the
120 transformation from a polymer to a cross-linked amorphous silicon network (i.e. Si-Si
121 bond construction) is particularly active between 300 and 360 $^\circ\text{C}$ and that the
122 amorphous network becomes more stable at higher temperature.

123

124 **3.2 Transformation from polydihydrosilane to a-Si:H film**

125 In 3.2.1, we study T_p -dependence of Raman spectra of amorphous phonon bands to
126 confirm the formation of the three-dimensional amorphous silicon network. In 3.2.2 the
127 quality of Sol.P a-Si:H films (voids and hydrogen/oxygen content) is discussed on the
128 basis of the infrared microstructure factor [2,11,12] and of the impurity content
129 measured by SIMS.

130 **3.2.1 Raman scattering**

131 Figs. 3(a) and 3(b) show the first-order Raman spectra of the Sol.P films prepared
132 at T_p in the range of 270–330 °C and 330–420°C, respectively. The Raman data were
133 averaged over 10 measurements for each sample in a back scattering geometry using a
134 He-Ne laser line (633 nm). In Fig. 3(a), typical phonon bands of a-Si:H [13,14] are
135 visible at $T_p = 330$ °C whereas films prepared at $T_p = 270$ and 300 °C show no clear
136 peaks corresponding to the amorphous silicon phonon bands. In literature, the a-Si:H
137 Raman phonon bands at 476, 387, 288, and 154 cm^{-1} have been assigned to transverse
138 optical (TO), longitudinal optical, longitudinal acoustic, and transverse acoustic band,
139 respectively. Fig. 3(b) shows the Raman spectra of the Sol.P films prepared at $T_p = 330$,
140 360, 390, and 420 °C, where the intensity was normalized to the same TO height. The
141 full width at half maximum (FWHM) of the TO band versus T_p is plotted in Fig. 3(c).

142 The appearance of amorphous silicon phonon bands for films prepared at $T_p \geq$
143 330 °C suggests construction of the three-dimensional amorphous silicon network near
144 the temperature $T_p = 330$ °C. Indeed, the Raman spectra for the Sol.P films prepared at
145 $T_p \geq 330$ °C are quite similar to typical Raman spectra for vacuum-processed (Vac.P)
146 a-Si:H films [13,14]. Thus one may term the Sol.P films prepared at $T_p \geq 330$ °C Sol.P
147 a-Si:H films. Our observed FWHM of the TO band in Fig. 3(c) shows a decrease from
148 80.5 to 71.5 cm^{-1} when T_p is increased from 300 to 420 °C. The decrease of the FWHM
149 indicates the improvement of short-range tetrahedral ordering because of its sensitivity
150 to the bond-angle fluctuations [14], so that the pyrolysis at $T_p \geq 330$ °C induces a
151 modification of the amorphous network from a more distorted to a more ideal
152 tetrahedral configuration, in addition to the amorphous silicon network construction.

153

154 3.2.2 FT-IR and SIMS

155 Figs. 4(a) and 4(b) show the IR absorption coefficient $\alpha(\omega)$ in the wavenumber
156 range of 1950–2200 cm^{-1} and 550–750 cm^{-1} , respectively, for the Sol.P films prepared
157 at $T_p = 270\text{--}420$ °C. The absorption peaks near 2000 and 2070–2090 cm^{-1} at $T_p \geq$
158 360 °C are assigned to the stretching modes of Si-H bonds embedded in bulk material
159 and to the stretching modes of Si-H/Si-H₂ bonds at void surface, respectively [11]. The
160 absorption band near 640 cm^{-1} in Fig. 4(b) is attributed to the Si-H wagging mode [15]
161 which is known to have a vibrational frequency near 640 cm^{-1} . Only the sample
162 prepared at 270 °C deviates significantly from this value. As is seen in Fig. 4(a), the
163 Si-H stretching modes of our material are all centered near 2080 cm^{-1} except for the
164 samples prepared at the rather low temperatures of 270 and 300 °C which show a Si-H
165 stretching absorption shifted to higher wavenumber.

166 As mentioned above, the 2070–2090 cm^{-1} peaks at $T_p \geq 330$ °C are related to the
167 vibration of Si-H/Si-H₂ bonded on external and internal void surfaces and the 2000 cm^{-1}
168 peak is attributed to Si-H vibrations in the bulk. Thus one may evaluate the sample
169 quality by using the infrared microstructure factor R [2,11,12],

$$170 R = I_{2090}/(I_{2000}+I_{2090}). \quad (1)$$

171 Here, I_{2090} and I_{2000} are integrated intensities of each oscillation modes near 2070–2090
172 and 2000 cm^{-1} , respectively. From the spectral data in Fig. 4(a), the estimated R ranges
173 from 0.91 ($T_p = 360$ °C) to 0.80 ($T_p = 420$ °C) whereas it is known that device-grade
174 Vac.P a-Si:H films show $R < 0.2$ [11,12] because of the domination of 2000 cm^{-1} peak.
175 Large values of R for our films imply a void-rich structure. Although the origin of peak
176 shift at $T_p \leq 330$ °C is not clear, it may be related to the oxidization or the change of
177 local environment of the Si-H dipole [16,17]. This suggests that the films prepared at T_p
178 ≤ 330 °C have quite poor quality.

179 To examine the degree of hydrogenation as well as the oxidation in our Sol.P films,
180 we determine the hydrogen and oxygen concentration using FT-IR and SIMS
181 measurements. Fig. 5 shows hydrogen and oxygen content as a function of T_p in which
182 the closed circles and squares are, respectively, hydrogen and oxygen content obtained
183 by SIMS measurement. The open circles show N_H/N_{Si} by FT-IR in which the density of
184 silicon is assumed to be $N_{Si} = 5 \times 10^{22}$ cm^{-3} . The density of hydrogen N_H is evaluated

185 from $\alpha(\omega)$ in Fig. 4(b) using Eq. (2) with the proportional constant $A_{640} = 2.1 \times 10^{19}$
186 cm^{-2} [18],

$$187 \quad N_H = A_{640} \int \frac{\alpha(\omega)}{\omega} d\omega. \quad (2)$$

188 Since the hydrogen content in polydihydrosilane is 67 at.%, the hydrogen
189 concentration values of 9.2–10.6 at.% (by SIMS) in films prepared at $T_p \geq 360$ °C
190 indicate a remarkable reduction in the hydrogen content during the pyrolysis. The
191 void-rich structure concluded from the large R value in films prepared at $T_p \geq 360$ °C is
192 presumably due to the three-dimensional shrinkage related to the weight loss. With
193 regard to oxygen, the high concentration of it for the films prepared at $T_p \leq 330$ °C
194 means that the construction of the amorphous silicon network is not dense enough so
195 that it oxidises rather easily in air.

196

197 **3.3 Relationship between TG/DTA and Raman/IR data**

198 In this section we discuss the relationship between the TG/DTA results and the
199 changes of the Raman and FT-IR spectra with rising preparation temperature and
200 speculate about the formation of the amorphous silicon network. Our previous TDS
201 results [3] indicated that Si-Si bonds in polydihydrosilane start to break near 280 °C
202 followed by breaking of Si-H bonds at near 300 °C. Since the breaking of Si-H bonds in
203 the polydihydrosilane is necessary for formation of the three-dimensional amorphous
204 silicon network, this network apparently is forming at temperature exceeding 300 °C.

205 The decrease in the TG curve from 25 to 280 °C and the positive DTA curve in Fig.
206 2 indicate that the breaking and reconstruction of Si-Si bonds proceeds locally even at
207 temperatures less than 280 °C. The drastic change of TG (visible in a peak in DTG)
208 between 270 and 360 °C suggests a release of high amounts of H_2 and SiH_x due to the
209 thermal decomposition of molecules via the breaking of Si-H and Si-Si bonds. The
210 broad exothermal peak in DTA near 320 °C likely corresponds to the construction of the
211 three-dimensional silicon network due to formation of Si-Si bonds and release of
212 hydrogen. The construction of the three-dimensional amorphous silicon network and the
213 strong reduction of the hydrogen content are confirmed by the Raman data (Fig. 3) and
214 by the FT-IR and SIMS results as shown in Fig. 5.

215

216 **3.4. Influence of pyrolysis on the electrical properties of Sol.P a-Si:H films**

217 **3.4.1 Optical gap**

218 Fig. 6 shows results of absorption measurements in the UV–visible range of Sol.P
219 films prepared at $T_p = 300$ to 420 °C. The data are depicted in a Tauc plot [19] as

$$220 (\alpha E)^{1/2} = B^{1/2}(E - E_g), \quad (3)$$

221 where α is the optical absorption coefficient, E is the photon energy in eV, B is a
222 constant, and E_g is the optical gap (called “Tauc gap”). The fitting procedure yields $E_g =$
223 2.40 , 1.92 , 1.64 , 1.64 , and 1.64 eV for the film prepared at $T_p = 300$, 330 , 360 , 390 , and
224 420 °C, respectively, as shown in Fig. 6(b). The parameter B is found to be 5.7×10^5
225 and 7.7×10^5 eV⁻¹cm⁻¹ for $T_p = 300$ and 330 °C, and 6.7×10^5 eV⁻¹cm⁻¹ for $T_p \geq$
226 360 °C. It is known that E_g in Vac.P a-Si:H films varies with the hydrogen content [2].
227 Accordingly, the T_p -dependence of E_g in Fig. 6(b) can be understood by the
228 dehydrogenation during pyrolysis as shown in Fig. 5. For T_p exceeding 360 °C the
229 absorption is no longer dependent on the hydrogen content, and gives $E_g = 1.64$ eV. This
230 is consistent with $E_g = 1.5$ – 1.6 eV observed in Vac.P unhydrogenated amorphous silicon
231 films [2,20].

232

233 **3.4.2. Conductivity and spin density**

234 Typical values of σ_d , σ_p and N_S at room temperature are plotted in Fig. 7 as a
235 function of T_p . With rising T_p from 300 to 330 °C, σ_d increases slightly, followed by a
236 drastic decrease at $T_p = 360$ °C, and attains 5.1×10^{-11} S/cm at $T_p = 420$ °C, while σ_p is
237 of the order of 10^{-7} S/cm, except for the minimum at $T_p = 360$ °C. The value of N_S
238 starting from 2.5×10^{16} cm⁻³ exhibits a maximum in a film prepared at $T_p = 360$ °C, and
239 attains 2.8×10^{17} cm⁻³ for the high- T_p films. Since the paramagnetic spin density
240 corresponds to the concentration of dangling bonds which act as a trapping site, the
241 reduction of N_S may lead to the increase of σ_p [21]. The increase of N_S in the range from
242 $T_p = 300$ to 360 °C is attributed mainly to the increase of dangling bonds due to the
243 breaking of the Si-H and Si-Si bonds. In contrast, the decrease of N_S in the range from
244 $T_p = 360$ to 420 °C suggests that the high T_p serves as an annealing effect to reduce the
245 number of dangling bonds (See also the FWHM data in Fig. 3(c)). A photosensitivity
246 (i.e. ratio of σ_p to σ_d) of Sol.P films prepared at $T_p \geq 360$ °C exhibits the order of 10^3 ,

247 whereas that of device-grade Vac.P a-Si:H films show 10^5 – 10^6 [2,22]. This low
248 photosensitivity indicates a rather poor quality of our films presumably related to the
249 high value of $N_S > 10^{17} \text{ cm}^{-3}$ for $T_p \geq 360$ °C. Note that device-grade Vac.P a-Si:H films
250 are known to have $N_S < 10^{16} \text{ cm}^{-3}$ [2].

251

252 **4. Conclusion**

253 In this study, we have emphasized that the pyrolytic transformation from
254 polydihydrosilane to amorphous silicon near 300–360 °C plays an essential role for the
255 formation of a Sol.P a-Si:H films. The drastic changes of Raman spectra between $T_p =$
256 300 and 330 °C give evidence for the construction of a three-dimensional amorphous
257 silicon network in this temperature range, as supported also by the TG/DTA results. The
258 electrical properties of the Sol.P a-Si:H films are much affected by the pyrolytic
259 transformation from a polymer to a-Si:H. Compared to device-grade Vac.P a-Si:H films
260 [2], the spin density is larger by one order of magnitude, and the photosensitivity is
261 smaller by one to two orders of magnitude. The infrared absorption of the Si-H
262 stretching modes indicates a void-rich material. Further work appears necessary to
263 improve the Sol.P a-Si:H material with the aim of fabrication of a-Si:H solar cells from
264 liquid phase precursors.

265

266 **Acknowledgements**

267 We thank Prof. S. Katayama for his discussion and valuable comments in the
268 present work. This study was funded by the Exploratory Research for Advanced
269 Technology (ERATO) program of Japan Science and Technology Agency.

270

271 **References**

- 272 [1] R. A. Street, Hydrogenated Amorphous Silicon, Cambridge University Press,
273 Cambridge, 1991.
- 274 [2] A. Shah, W. Beyer, in: A. Shah (Ed.), Thin-Film Silicon Solar Cells, EEPL Press,
275 2010, pp. 17–96.
- 276 [3] T. Shimoda, Y. Matsuki, M. Furusawa, T. Aoki, I. Yudasaka, H. Tanaka, H. Iwasawa,
277 D. Wang, M. Miyasaka, and Y. Takeuchi, Nature 440 (2006) 783.

278 [4] T. Masuda, N. Sotani, H. Hamada, Y. Matsuki, and T. Shimoda, Appl. Phys. Lett.
279 100 (2012) 253908.

280 [5] M. Fujiki, Y. Kawamoto, M. Kato, Y. Fujimoto, T. Saito, S. Hososhima, and G.
281 Kwak, Chem. Mater. 21 (2009) 2459.

282 [6] T. Masuda, Y. Matsuki, and T. Shimoda, Polymer 53 (2012) 2973.

283 [7] F. S. Kipping, J. Chem. Soc. 125 (1924) 2291.

284 [8] E. Hengge, and G. Bauer, Angew. Chem. Internat. ED. 12 (1973) 316.

285 [9] T. Masuda, Y. Matsuki, and T. Shimoda, Thin Solid Films 520 (2012) 5091.

286 [10] T. Masuda, Y. Matsuki, and T. Shimoda., J. Colloid Interface Sci. 340 (2009) 298;
287 note that optical band gap of polydihydrosilane was estimated by using $E_g = \hbar\omega_{UV}$, with
288 ω_{UV} being the observed ultraviolet absorption frequency. .

289 [11] J. Mullerova, P. Sutta, G. v. Elzaker, M. Zeman, and M. Mikula, Appl. Surf. Sci.
290 254 (2008) 3690.

291 [12] E. Bhattacharya and A. H. Mahan, Appl. Phys. Lett. 52 (1988) 1587

292 [13] T. Ishidate, K. Inoue, K. Tsuji and S. Minomura, Solid State Commun. 42 (1982)
293 197.

294 [14] D. Beeman, R. Tsu, and M. F. Thorpe, Phys. Rev. B 32 (1985) 874.

295 [15] M. H. Brodsky, M. Cardona, and J.J. Cuomo, Phys. Rev. B 16(8) (1977) 3556.

296 [16] G. Lucovsky, J. Yang, S. S. Chao, J. E. Tyler, and W. Czubytyj, Phys. Rev. B 28
297 (1983) 3225.

298 [17] M. Cardona, Phys. Stat. Sol. (b) 118 (1983) 463.

299 [18] A. A. Langford, M. L. Fleet, B. P. Nelson, W. A. Lanford, and N. Maley, Phys. Rev.
300 B 45 (1992) 13367.

301 [19] J. Tauc, R. Grigorovici, and A. Vancu, Phys. Stat. Sol. 15 (1966) 627.

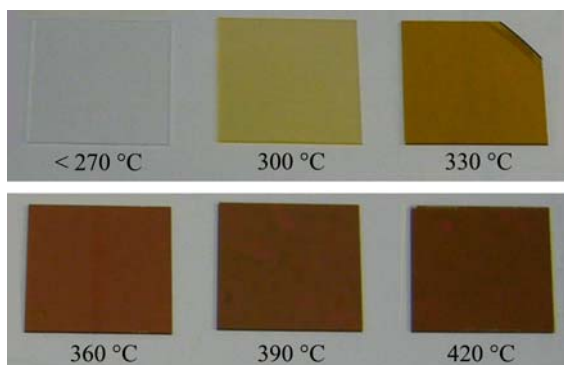
302 [20] Y. Ashida, Y. Mishima, M. Hirose, Y. Osaka, and K. Kojima, Jpn. J. Appl. Phys. 23
303 (1984) L129.

304 [21] H. Dersch, L. Schweitzer, and J. Stuke, Phys. Rev. B 28 (1983) 4678.

305 [22] W. Beyer and B. Hoheisel, Solid State Commun. 47 (1983) 573.

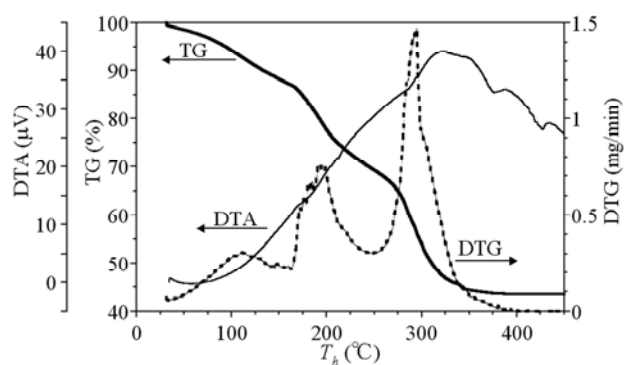
306

307



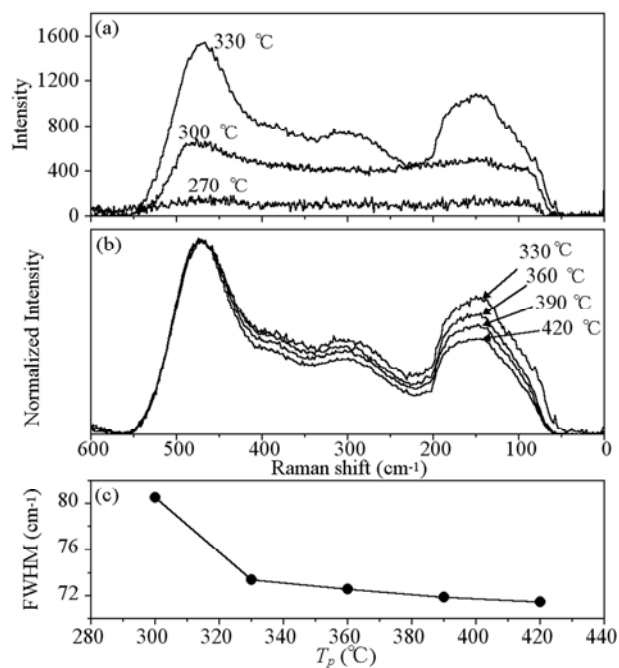
308

309 Fig. 1 Photographic image of Sol.P films coated on quartz substrate. The films were
310 pyrolysed at $T_p = 270\text{--}420$ °C. Substrate size is 2×2 cm².



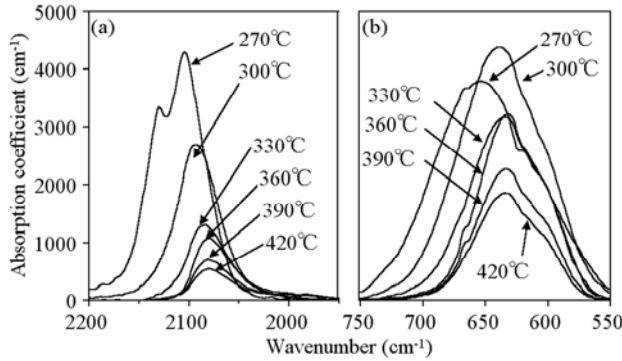
311

312 Fig. 2 TG (bold solid line), DTA (thin solid line), and DTG (dashed line) curves of
313 polydihydrosilane as a function of heating temperature.

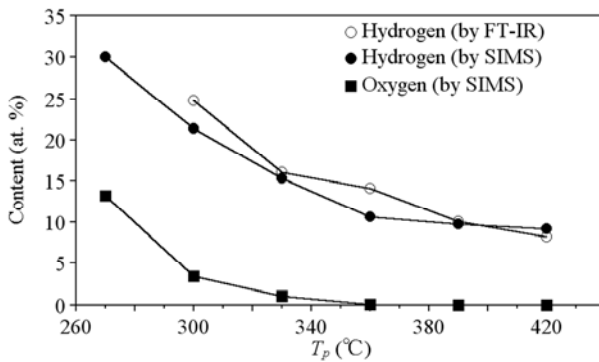


314

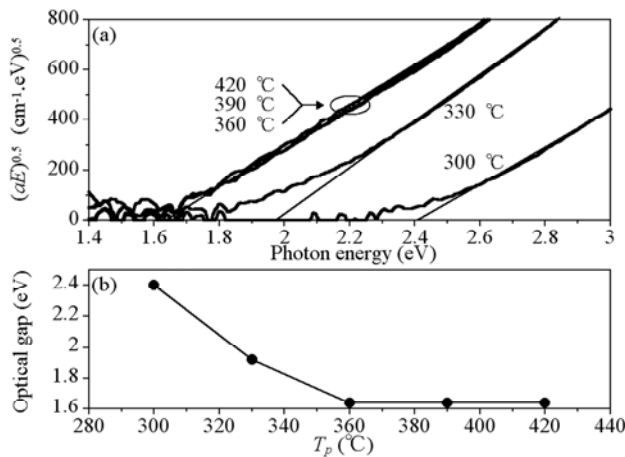
315 Fig. 3 (a) Raman spectra from the Sol.P films prepared at $T_p = 270, 300,$ and 330 °C. (b)
 316 Raman spectra from the films prepared at $T_p = 330, 360, 390,$ and 420 °C. The intensity
 317 was normalized to the same TO height. (c) FWHM of the TO Raman band versus T_p .



318
 319 Fig. 4 FT-IR absorbance spectra at (a) $1950\text{--}2200\text{ cm}^{-1}$ and (b) $550\text{--}750\text{ cm}^{-1}$ for Sol.P
 320 films prepared at $T_p = 270\text{--}420$ °C on single crystalline silicon substrates.

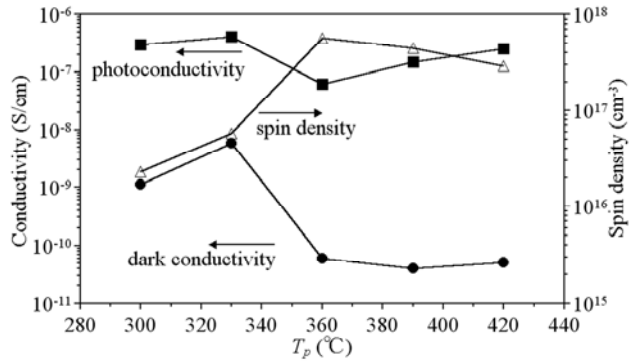


321
 322 Fig. 5 Hydrogen and oxygen content versus T_p . The closed circles and squares give the
 323 hydrogen and oxygen concentrations, respectively, from SIMS measurements. The open
 324 circles give the hydrogen content estimated from the IR absorption data analyzing the
 325 wagging mode near 640 cm^{-1} .



326

327 Fig. 6 (a) Tauc plot of the Sol.P films on a quartz substrate. The films were prepared at
 328 $T_p = 300\text{--}420\text{ }^\circ\text{C}$. (b) Plot of E_g versus T_p .



329
 330 Fig. 7 Conductivity and spin density in Sol.P films prepared at $T_p = 300\text{--}420\text{ }^\circ\text{C}$. The
 331 value of σ_d and σ_p at room temperature and of N_S are depicted by closed circles, closed
 332 squares, and open triangles, respectively.